



## Theoretical Models of the Effect of Flow Regulating Additives

Sultanov Sahib Sobirovich <sup>1</sup>

<sup>1</sup> Independent student of the Academy of the Ministry of Emergency Situations of the Republic of Uzbekistan

**Abstract:** Various theoretical models are used to illustrate the essential principles of the effect of additives on powder flow, in which guest particles diminish the adhesion (mutual attraction) forces between big host particles. Non-deformable solid spheres of ideal shape may be included in models.

Rumpf proposed a simple model to describe the lowering of the adhesion force operating across uneven surfaces - a flat plate with thickness  $a$  and a sphere with radius  $R$ . (Fig. 1). Surface imperfections are modeled in this model by a hemisphere of radius  $r$  adsorbed on the surface of a bigger sphere. According to this method, the decrease in contact forces has a distinct reliance on the radius of the hemisphere. The force of interaction between two big particles declines and eventually reaches a minimum as the adsorbed hemisphere rises. The interaction forces grow with the size of the adsorbed hemisphere.

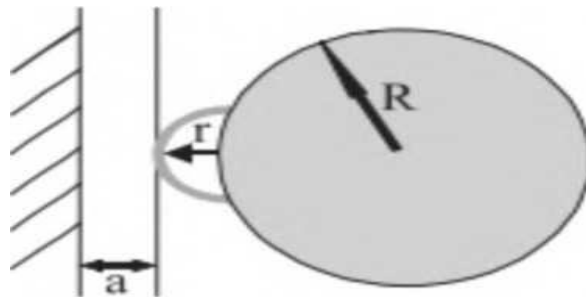


Figure 1. Schematic representation of the Rumpf model

The van der Waals force can be calculated using the following equation (1), the left part of which describes the interaction between the sphere and the plate, while the right part describes the interaction between the hemisphere and the plate:

$$F_{vdw} = \frac{C_H}{6} \left[ \frac{R}{(a+r)^2} + \frac{r}{a^2} \right] \quad (1)$$

The Rabinovich model (Figure 2) describes the interaction between a spherical particle and a hemisphere of roughness.

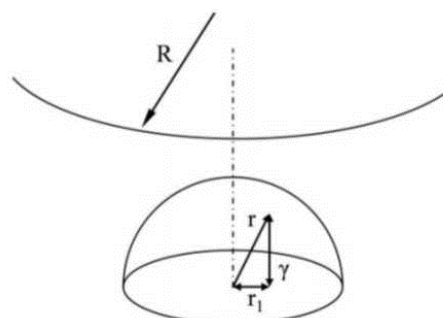


Figure 2. A schematic representation of the Rabinovich model

The radius of a semicircle is calculated using the following equation:

$$r_{ms} = \sqrt{\frac{K_p}{\lambda^2}} \cdot 32 \int_0^r \gamma^2 r_1 dr_1 \quad (2)$$

here  $r_1$  and  $\gamma$  - the radius of the hemisphere is the lengths of the sides forming a right triangle.  $\lambda$  - the distance between the hemispheres,  $K_p$  - the location density of the hemispheres on the surface. If it is assumed that  $\lambda = 4r$  and  $K_p = 0.907$ , then  $r_{ms} = 0.673r$ .

The van der Waals force can be calculated by the following equation (3), where  $K_1$  is the proportionality coefficient between  $K_p$  and  $\gamma$ :

$$F_{vdW} = \frac{C_H R}{6a^2} \left[ \frac{1}{1 + \frac{32Rk_1 r_{ms}}{\lambda^2}} + \frac{1}{1 + \left(\frac{k_1 r_{ms}}{a_0}\right)^2} \right] \quad (3)$$

The difference of the Eber model (Fig. 3) consists in replacing the hemispherical roughness with a spherical particle of the guest.

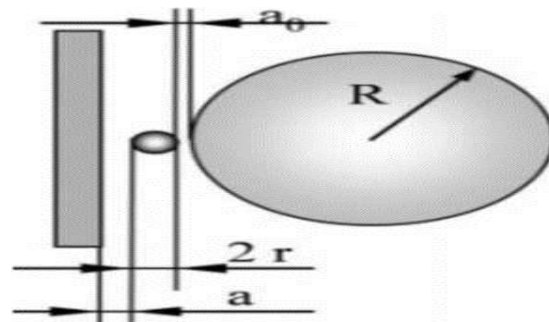


Figure 3. Schematic representation of Eber's model

The model has been modified to better reflect the reduction of powder adhesion forces utilizing nanoparticles. In this situation, the connections must be seen (studied) in two cases: the connection of the host particle with the visitor particle and the connection of the guest particle with the flat plate. The smallest contact distance is 0.4 nm, which is substantially smaller than the average size of nanoparticles (mostly 10 nm). As a result, this distance can be neglected, and Eber developed the following formula for the Van der Waals force:

$$F_{vdW} = \frac{C_H}{6} \left[ \frac{R}{(a + 2r)^2} + \frac{r}{a^2} \right] \quad (4)$$

The Zimmerman model describes the interaction of two host particles and one guest particle. As an improvement of the Rumpf and Eber models, the parameters of all distances between the host and guest particles - the average radius  $R_{1,2}$  - were added to the model (Fig. 5).

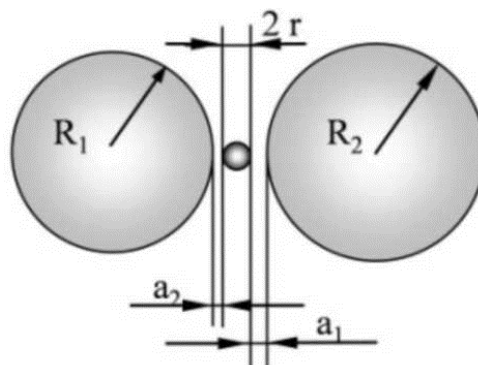


Figure 4. A schematic representation of the Zimmerman model

The inclusion of a small sphere representing a guest particle that governs the powder flow results in a considerable drop in the Van der Waals force (5). As the equation shows, the larger the radius of the massive particles, the more pronounced the reduction in contact forces.

$$F_{vdW} = \frac{C_H}{6} \left[ \frac{R_1 r}{a^2 (R_1 + r)} + \frac{R_{1,2}}{(a_1 + a_2 + 2r)^2} \right] \quad (5)$$

Because the conditions of the models described above, which involve only one roughness hemisphere and one guest particle, are far from reality, models that account for the presence of several roughnesses in the junction area have been devised.

The host and guest particles are supposed to be made of the same material in the Paul and Vick model, and the hemispheres represent rough particle asperities or nanoparticles adsorbed on the surface. In the junction zone, they form six distinct geometrical positions (Fig. 6).

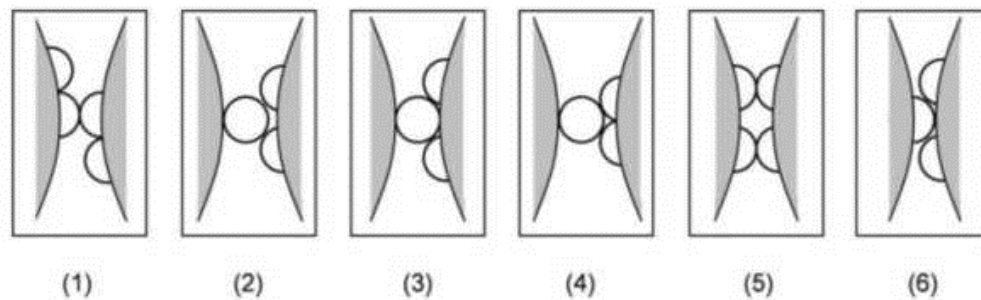


Figure 5. Possible options for the location of irregularities in the junction area according to the model of Paul and Vick

The van der Waals force is calculated by the following equation:

$$F_{vdW} = \frac{C_H}{6} \left[ \frac{R_{1,2}}{(a + r_{\max})^2} + \sum_{i=1}^{N_k} \frac{r_i R_i}{a^2 (r_i + R_i)} \right] \quad (6)$$

here:  $R_i$  -  $i$  is the roughness radius,  $r_{\max}$  - the largest roughness radius and  $N_k$  - the number of asperities within the junction zone. The left portion of the formula explains the interaction between the host particles, whereas the right part describes the sum of all interactions in the junction zone between the asperities and the host particles.

The Meier model, which is based on a stable three-point junction with adsorbate nanoparticles firmly packed at the extremities of an equilateral triangle, theoretically represents the decrease in the strength of interaction between particles as their surface area is covered by adsorbate nanoparticles (Fig. 7). The model can calculate the distance between interacting powder particles as well as the strength of their Van der Waals interaction. This model simply covers two opposing scenarios, divided by the value of the hazardous surface cover. A robust contact process occurs between the powder particles up to this value. The nanoparticles then enter the space (crack) between the host particles, and the short-range adhesion force is eliminated altogether.

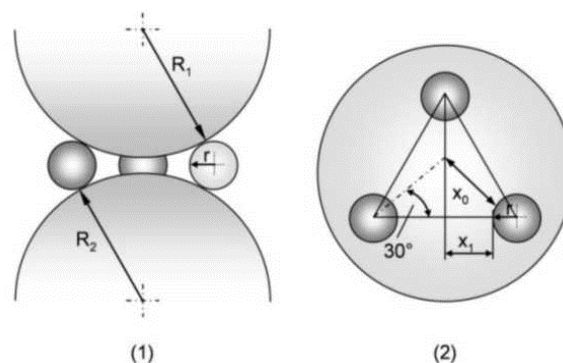


Figure 6. Schematic representation of Meyer's model.

The geometric distance  $\gamma$  between the host particles is calculated by the following equation:

$$\gamma = 2 \left[ \sqrt{(R+r)^2 - \frac{4}{3}(x_1+r)^2} - R \right] \quad (7)$$

here  $x_1$  - distance between two guest particles.

Then the Van der Waals force is calculated according to the following formula:

$$F_{vdW} = \frac{C_H}{6} \left[ \frac{R_{1,2}}{\gamma^2} + 3 \frac{Rr}{(R+r)a^2} \right] \quad (8)$$

here  $R_1$  and  $R_2$  radius of host particles and  $r$  is the radius of the guest particle.

The Kurfess model adds to and corrects the Meyer model, better reflecting the flow-regulating influence of nanoparticles on interparticle interaction forces. The model describes the free covering of powder particle surfaces and contains the following steps:

- 1) Adsorbate-free powder particle coating - powder particles are freely and successively coated with nanoparticles. The model allows for nanoparticle coating.
- 2) Using three nanoparticle dots, two powder particles are placed to produce stable bonding. A coated powder particle collides with an uncoated powder sphere. A huge uncoated powder particle rolls over the adsorbates until a stable contact is achieved at three locations.
- 3) Determine the Van der Waals force by adding all interaction findings from the Hamaker model.

$\vec{a}_i$  coordinates describe the center of positions (locations) of adsorbates on the surface of the host particle,  $R$ - radius of host particles,  $r$ - total radius of all nanoadsorbates,  $A_{HH}$  and  $A_{AH}$  Hamaker constants for the interaction between host and adsorbate particles. Taking into account the vector sum of all host-particle interactions, the Van der Waals force equation has the following form:

$$\vec{F}_{vdW} = - \frac{A_{HH}}{6 \left( \left| \vec{S} \right| - 2R \right)^2} \cdot \frac{R}{2} \cdot \frac{\vec{S}}{\left| \vec{S} \right|} - \sum_{i=1}^{N_A} \frac{A_{AH}}{6 \left( \left| \vec{S} - \vec{a}_i \right| - r - R \right)^2} \cdot \frac{\vec{S} - \vec{a}_i}{\left| \vec{S} - \vec{a}_i \right|} \quad (9)$$

When computing the interaction force, such a model provides for a more realistic continuous decreasing curve of the interaction force between powder particles as a function of the powder particles' surface covering.

Unlike the Meyer model, which produces a step-like curve, the Kurfess model improves the prediction of mutual attraction force reduction from the covering area and allows for the generation of a continuous curve. Furthermore, scaling laws independent of the materials utilized were determined by adjusting the parameters.

When the coverage area is  $q=0$ , there are no nanosized adsorbates on the surface of the host particles, and the forces appear solely as a result of host particle interaction. The experimentally measured mutual attraction exhibits higher values than the estimated data, but has a qualitatively similar sort of curve. This validates the Kurfes model approach for predicting host particle interactions when their surface is coated with guest particles. The disparity between the experimental and predicted results is explained by capillary forces and the production of nanoparticle aggregates.

## References:

1. Брушлинский Н.Н., Копыловт Н.П., Усманов М.Х. и др. Новые огнезащитные и аварийно-спасательные устройства// Пожарное дело.–2003.Вып. 5.–С. 38–40.

2. Отчеты по НИР “Анализ действий пожарной охраны при тушении крупных пожаров и проведении связанных с ними аварийно–спасательных работ на территории Российской Федерации, ВНИИПО. 2000–2016 гг.
3. Лапшин Д.Н., Кунин А.В., Смирнов С.А., Ильин А.П. Химическая промышленность сегодня// 2014. № 3. с.31–38.
4. Р.Б.Болтабоев, И.Р.Толибжонов “Ёнғинларни ривожланиши ва ўчиришнинг физик–кимёвий асослари”// Ўзбекистон Республикаси ИИВ Ёнғин хавфсизлиги институти 2018 й.
5. STIF international association of fire and rescue services 2007 №12
6. Яковенко Ю. Ф. Россия: пожарная охрана на рубеже веков// – М.: «СИБЕР», 2004. – 208 с.
7. Лапшин Д.Н., Кунин А.В., Смирнов С.А., Ильин А.П., Беловошин.А.В. Пожаровзрывобезопасность,// 2012. Т. 21. № 1. с.83–87.